

Phase Diagram of the First-Order Vortex-Core Transition in Superfluid $^3\text{He-B}$

J. P. Pekola, J. T. Simola, P. J. Hakonen, M. Krusius, O. V. Lounasmaa, and K. K. Nummilla
Low Temperature Laboratory, Helsinki University of Technology, SF-02150 Espoo 15, Finland

and

G. Mamniashvili
*Institute of Physics, Georgian Academy of Sciences, 380077 Tbilisi,
Union of Soviet Socialist Republics*

and

R. E. Packard
Department of Physics, University of California, Berkeley, California 94720

and

G. E. Volovik
*L. D. Landau Institute for Theoretical Physics, U.S.S.R. Academy of Sciences, 117334 Moscow,
Union of Soviet Socialist Republics*
(Received 13 June 1984)

The phase diagram of quantized vortices in $^3\text{He-B}$ has been obtained with two techniques. Our NMR measurements show that magnetization displays a pressure-dependent first-order phase change at $T_V(P)$. Our gyroscopic experiments reveal a transition curve $T_G(P)$ which marks an abrupt change in the critical velocity. Both curves show a weak magnetic field dependence, run similarly in the (P, T) plane, and seem to mark the same vortex-core transition.

PACS numbers: 67.50.Fi

Earlier measurements¹⁻³ at $P = 29.3$ bars and $H = 284$ G revealed a discontinuity in the rotation-induced NMR frequency shift at $T_V = 0.6T_c$, identified as a first-order phase transition in the core structure of quantized vortices. We have now extended these experiments to other pressures and fields to establish the curve separating the two different types of vortices in the (P, T) plane. We have also continued our gyroscopic experiments⁴ and now can make a rather detailed report on the phase transition, manifested by a discontinuous change in the critical flow velocity v_c and by a large latent heat.

Our measurements were carried out in a rotating nuclear demagnetization refrigerator.⁵ The NMR cell² of open cylindrical geometry is 5 mm in diameter and 30 mm long. The heart of the gyroscope experiment⁴ is a torus, of radius $R = 22$ mm, packed with 20- μm plastic powder.

An NMR result is illustrated in Fig. 1. The rotation-induced frequency shift $\Delta\nu$ exhibits a discontinuity at $T_V = 0.6T_c = 1.6$ mK. The jump in $\Delta\nu$ is proportional to Ω , the angular velocity of rotation, while T_V is independent of Ω . Such a behavior rules out all textural transitions in the

bulk liquid, leaving only a phase change inside the vortex cores as an explanation. The latter is insensitive to Ω because only at $\Omega > 10^5$ rad/s does the distance between vortices become small enough to disturb the core structure, while the jump in $\Delta\nu$ is proportional to the density of vortices $n_V = (4m_3/h)\Omega$.

The influence of the vortex cores on the NMR shifts, observed both in axial, $\vec{H} \parallel \vec{\Omega}$, and in tilted magnetic fields, are well accounted for by the extra vortex terms, $\frac{2}{5}a\lambda(\hat{\Omega}_i R_{ik} H_k)^2$ and $\frac{4}{5}a\kappa(\hat{\Omega}_i R_{ik} \times H_k)$, in the textural free energy. Here a is a measure of the small magnetic anisotropy energy in bulk liquid, $-a(\hat{n} \cdot \vec{H})^2$, and $R_{ik}(\hat{n})$ is a matrix representing a rotation around the anisotropy axis \hat{n} by the angle $\cos^{-1}(-\frac{1}{4})$. Phenomenological constants λ and κ , associated with the large magnetic anisotropy and with the spontaneous magnetization in the vortex-core region, respectively, are manifested by odd and even NMR shifts, in respect to \vec{H} and $\vec{\Omega}$.

Prominent discontinuities, $\Delta\lambda = (0.1-0.25)\Omega$ s/rad and $\Delta\kappa/H = -(0.002-0.02)\Omega$ s/rad, were observed during warmup at the vortex-core transition. The magnitudes of these discontinuities scale

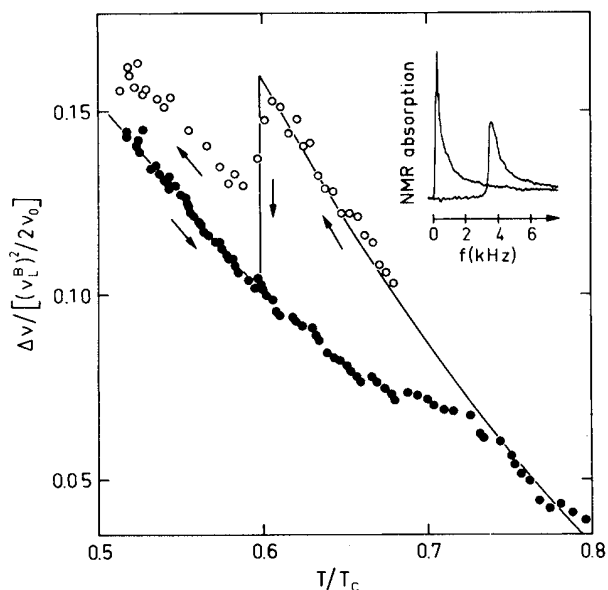


FIG. 1. The NMR frequency change $\Delta\nu$ (normalized by the maximum frequency shift in $^3\text{He-B}$) as a function of the reduced temperature. In this measurement, at $P = 29.3$ bars, $H = 284$ G, and $\angle(\vec{\Omega}, \vec{H}) = 25^\circ$, the cryostat was continuously rotated at $\Omega = 1.4$ rad/s during cooldown (open circles) and warmup (closed circles). The inset shows an example of the primary NMR absorption data at rest (left) and under rotation from which $\Delta\nu$ is obtained. Thermal hysteresis near $T_V = 0.6T_c$ becomes evident when the data points are compared with the solid curve showing the measured equilibrium behavior.

with Ω but the transition temperature T_V is independent of Ω .⁶ The phase boundary $T_V(P)$, defined by the jump in $\Delta\nu$, is shown in Fig. 2. Most of our NMR measurements were carried out at $H = 284$ G. Experiments were also made at 500 G under $P = 25.0$ bars and an increase of about 1% in T_V/T_c was seen. At the lowest pressure, $P = 17.1$ bars, the transition line was crossed twice, which indicates that $T_V(P)$ tends to curve towards higher pressures when approaching the superfluid phase transition curve $T_c(P)$.

Because the NMR frequency shifts vanish in proportion to $1 - T/T_c$ near T_c , the termination point of $T_V(P)$ has not been established, i.e., it may be on the $T_c(P)$ line or within the B phase. Some indication for the absence of a critical point is provided by the observation that $\Delta\lambda/\lambda$ does not start to decrease when $T_c(P)$ is approached along $T_V(P)$. We also wish to point out the thermal hysteresis associated with the vortex-core transition, as illustrated in Fig. 1; this proves the first-order nature of the observed phase change.

In our recent hydrodynamic measurements,⁴ where we used an ac gyroscope, two regimes with

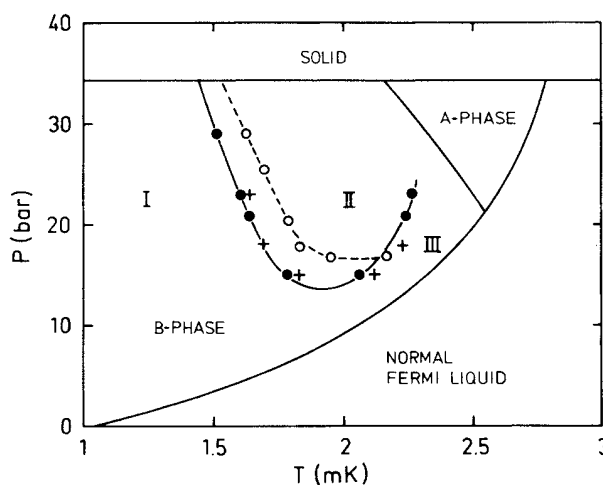


FIG. 2. Observed transitions on the phase diagram of rotating $^3\text{He-B}$: open circles, $H = 284$ G (NMR experiment); closed circles, $H = 0$; crosses, $H = 40$ G (gyroscopic experiment). Regions I, II, and III are discussed in the text.

distinct critical velocities were found at $P = 29.3$ bars. A careful study of the maximum persistable angular momentum L_c as a function of temperature, pressure, and magnetic field has now been made. Our experiments at a low (< 2 G) external field and at $H = 40$ G reveal a phase boundary $T_G(P)$ running in the (P, T) plane as shown in Fig. 2. $T_G(P)$ also has a weak dependence on H .

The discontinuous change observed in the critical velocity across the transition at T_G is illustrated in Fig. 3; data on L are shown from five different experiments. The sense of rotation always alternated between two successive measurements of L . After each preparative rotation Ω_p , the persistent angular momentum was measured with the cryostat at rest. According to our data, applying an $H = 40$ G field decreases the $v_c = 7$ mm/s critical velocity in region I (see Fig. 2) by only 10%. Unexpectedly, a stronger effect was observed in region II: v_c increases from 5–7 mm/s at $H = 0$ to 12–15 mm/s at 40 G under all pressures.

An equally striking feature of the transition at T_G is the large latent heat, $Q_G \approx (\Omega_p - \Omega_c) \mu\text{J}\cdot\text{s}/\text{mol}\cdot\text{rad}$, comparable to $Q_{BA} \approx 1.5 \mu\text{J}/\text{mol}$, the latent heat of the $B \rightarrow A$ transition under the melting pressure. Q_G was estimated from warm-up curves like those in Fig. 4. A latent heat was observed only in the presence of a persistent superflow $v_s \approx R(\Omega_p - \Omega_c)$.

The identification of the changes at T_G with the vortex-core transition requires the presence of remanent vorticity, which is a concept well established in He II.⁷ In our experiments, the remanent

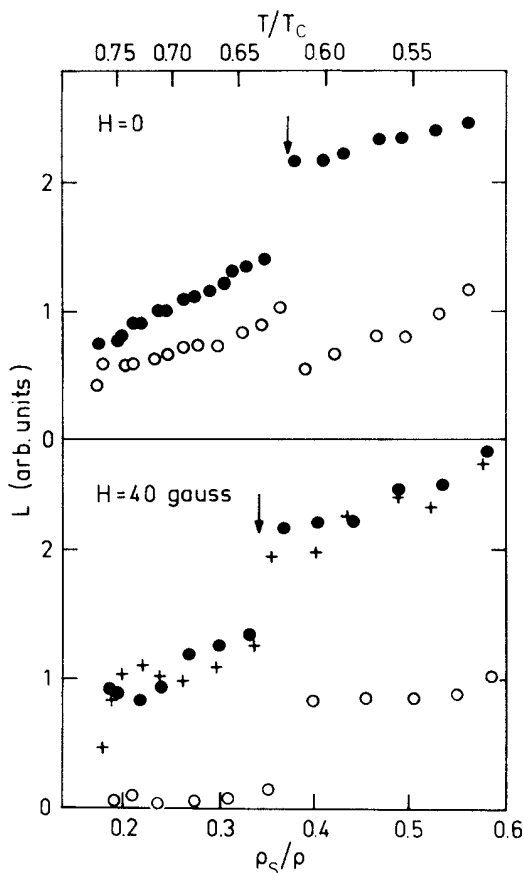


FIG. 3. The persistent angular momentum L as a function of reduced temperature T/T_c (upper scale) and the fraction of superfluid, ρ_s/ρ , in the cell. $P = 23.0$ bars, and the preparation angular velocities were (open circles) $\Omega_p = 0.40$ rad/s, and (closed circles and crosses) 0.86 rad/s. The transition in v_c is seen in all cases as an abrupt change in L . Arrows indicate the points at which a latent heat was observed.

vorticity $\text{curl} \vec{v}_s$, of the order of v_s/d , arises during the creation of superflow; vortices then become pinned to the $d \approx 20\text{-}\mu\text{m}$ -diam powder particles. This leads to the estimate $n_G \approx m_3 v_s / \hbar d$ for the density of vortex lines in the torus. The equilibrium vortex density n_V in our NMR cell of open geometry is 3 to 4 orders of magnitude less; this explains why Q_V was not observed.

If the latent heat is, indeed, due to a change in the condensation free energy F_{cond} of the vortex core, we obtain $Q_G \approx F_{\text{cond}} n_G \pi R_0^2$, which leads to the core radius $R_0 \approx 30\xi$, where $\xi \approx 10$ nm is the coherence length. This value of R_0 is still compatible with the estimate $R_0 \approx 10\xi$ from NMR experiments.² It is possible that n_G is enhanced by the complicated geometry of the powder.

As in He II,⁷ pinned vorticity acts as a nucleation

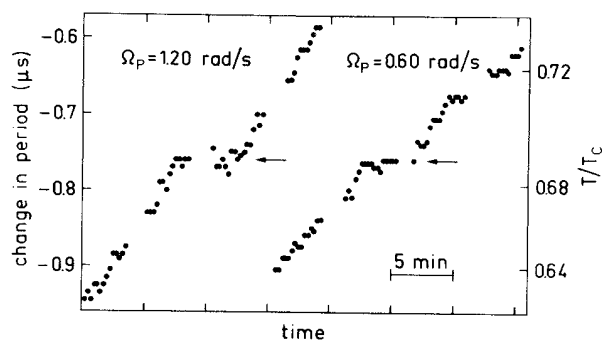


FIG. 4. Warmup curves of the gyroscope at two different values of Ω_p ; in this experiment $P = 18.0$ bars and $H = 40$ G. Under these conditions $\Omega_c = 0.35$ rad/s. The latent heat is clearly seen as a plateau in the warmup curves. The change in the gyroscope's resonant period, from that observed at T_c , increases towards lower temperatures because the amount of normal fluid in the torus decreases; we used this effect as our thermometric parameter (Ref. 4).

center for the growth of vortex rings when the Feynman critical velocity, $v_F = (\hbar/m_3 d) \ln(d/R_0) \approx 7$ mm/s, is reached. Our measured critical velocities are of the order of v_F . However, the difference of v_c in regions I and II shows that the process of vortex creation is more complicated. In regions I and III the onset of the persistent supercurrent was sharp at $\Omega = \Omega_c$, whereas in region II, especially in a magnetic field, the process was smoothed. This indicates that the creation of vortices depends on their core structure. For example, pinning should be different for the observed two types of vortices and it should depend on the external magnetic field. The growth rate of vortex rings of critical size is essentially determined by vibrations, as has been found for He II.⁸ It may be that the 40% decrease in the gyroscope's vibration intensity at $H = 40$ G, in comparison with $H = 0$, explains the puzzling increase of v_c in region II with field, observed at each pressure; we did not investigate, however, this effect in detail.

The observed clear, albeit small, differences between the T_V and T_G curves may be partly due to different calibrations of the thermometers at low temperatures. However, near T_c the influence of the magnetic field on the core structures becomes important.⁹ It is worth noting from Fig. 2 that the T_G data, corresponding to relatively low magnetic fields, do not approach the T_c curve. We could not find any evidence of additional transition lines emerging from the T_V or T_G curves. For example, gyroscopic experiments at $P = 12.0$ bars and $H = 0$ and NMR data at $P = 15.5$ bars and $H = 284$ G do

not reveal any signs of transition lines. Further, NMR experiments done at 17.1 bars and 284 G and gyroscopic measurements at 15.0 and 23.0 bars at $H=0$ show that, at each pressure, the λ vs T curves in regions I and III can be joined smoothly across region II and that v_c is the same in regions I and III. Therefore, the structures present in regions I and III are similar as far as λ and v_c are concerned.

At $H=0$ and near T_c there thus exists only one type of vortex. This is consistent with the recent theoretical result of Salomaa and Volovik.⁹ They found that there are five types of axially symmetric singly quantized vortices, which differ in their core structure. Numerical calculations show that at $H=0$ and in the Ginzburg-Landau regime near T_c only one of them is stable. This vortex, to be identified with that observed experimentally in regions I and III, has a core occupied by A -phase liquid, responsible for the susceptibility anisotropy, and by ferromagnetic β -phase liquid, with spontaneous magnetization. However, the detailed mechanisms leading to the vortex-core transition at T_V and the structure of the vortex in region II have not yet been unambiguously identified.

In summary, we note that the transitions at T_V and T_G show similar features: The jump in the NMR frequency shift and the discontinuity in v_c are both rotation induced but the transition temperatures are independent of Ω ; the similarity of the T_V and T_G curves in the (P, T) plane is obvious. We are thus dealing with the same vortex-core transition in both cases. If this conclusion is correct, our data provide some clues about the vortex gen-

eration process in $^3\text{He-B}$.

We wish to thank P. Kumar, J. Kurkijärvi, M. M. Salomaa, J. A. Sauls, and E. V. Thuneberg for discussions. Our work was supported by the Academy of Finland, the Wihuri Foundation, and the U. S. National Science Foundation through Grant No. DMR-81-19542.

¹O. T. Ikkala, G. E. Volovik, P. J. Hakonen, Yu. M. Bunkov, S. T. Islander, and G. A. Kharadze, Pis'ma Zh. Eksp. Teor. Fiz. **35**, 338 (1982) [JETP Lett. **35**, 416 (1982)].

²P. J. Hakonen, O. T. Ikkala, S. T. Islander, O. V. Lounasmaa, and G. E. Volovik, J. Low Temp. Phys. **53**, 425 (1983).

³P. J. Hakonen, M. Krusius, M. M. Salomaa, J. T. Simola, Yu. M. Bunkov, V. P. Mineev, and G. E. Volovik, Phys. Rev. Lett. **51**, 1362 (1983).

⁴J. P. Pekola, J. T. Simola, K. K. Nummilla, O. V. Lounasmaa, and R. E. Packard, Phys. Rev. Lett. **53**, 70 (1984).

⁵P. J. Hakonen, O. T. Ikkala, S. T. Islander, T. K. Markkula, P. Roubeau, K. M. Saloheimo, D. I. Garibashvili, and J. S. Tsakadze, Cryogenics **23**, 243 (1983).

⁶P. J. Hakonen, M. Krusius, G. Mamniashvili, and J. T. Simola, to be published.

⁷D. D. Awschalom and K. W. Schwarz, Phys. Rev. Lett. **52**, 49 (1984).

⁸S. J. Putterman, *Superfluid Hydrodynamics* (North-Holland, Amsterdam, 1974), pp. 262-266.

⁹M. M. Salomaa and G. E. Volovik, Phys. Rev. Lett. **51**, 2040 (1983), and to be published.